



Title	Inferring future changes in gene flow under climate change in riverscapes : a pilot case study in fluvial sculpin
Author(s)	Nakajima, Souta; Suzuki, Hiroaki; Nakatsugawa, Makoto; Matsuo, Ayumi; Hirota, Shun K.; Suyama, Yoshihisa; Nakamura, Futoshi
Citation	Landscape Ecology, 38, 1351-1362 <a href="https://doi.org/10.1007/s10980-023-01633-x">https://doi.org/10.1007/s10980-023-01633-x</a>
Issue Date	2023-03-15
Doc URL	<a href="http://hdl.handle.net/2115/91323">http://hdl.handle.net/2115/91323</a>
Rights	This version of the article has been accepted for publication, after peer review (when applicable) and is subject to Springer Nature 's AM terms of use, but is not the Version of Record and does not reflect post-acceptance improvements, or any corrections. The Version of Record is available online at: <a href="http://dx.doi.org/10.1007/s10980-023-01633-x">http://dx.doi.org/10.1007/s10980-023-01633-x</a>
Type	article (author version)
File Information	CottusRG.pdf



[Instructions for use](#)

1 **Inferring future changes in gene flow under climate change in riverscapes: a pilot case**  
2 **study in fluvial sculpin**

3

4 Souta Nakajima<sup>1,2,\*</sup>, Hiroaki Suzuki<sup>3,4</sup>, Makoto Nakatsugawa<sup>3</sup>, Ayumi Matsuo<sup>5</sup>, Shun K. Hirota<sup>5,6</sup>,  
5 Yoshihisa Suyama<sup>5</sup>, Futoshi Nakamura<sup>1</sup>

6

7 <sup>1</sup> Graduate School of Agriculture, Hokkaido University, Kita-ku N9W9, Sapporo, Hokkaido 060-8589,  
8 Japan

9 <sup>2</sup> Present address: Water Environment Research Group, Public Works Research Institute, Minamihara  
10 1-6, Tsukuba, Ibaraki 305-8516, Japan

11 <sup>3</sup> Graduate School of Engineering, Muroran Institute of Technology, Mizumoto-cho 27-1, Muroran,  
12 Hokkaido 050-8585, Japan

13 <sup>4</sup> Research Institute of Energy, Environment and Geology, Hokkaido Research Organization, Kita-ku  
14 N19W12, Sapporo, Hokkaido 060-0819, Japan

15 <sup>5</sup> Graduate School of Agricultural Science, Tohoku University, Yomogida 232-3, Naruko-onsen,  
16 Osaki, Miyagi 989-6711, Japan

17 <sup>6</sup> Present address: Botanical Gardens, Osaka Metropolitan University, Kisaichi 2000, Katano, Osaka  
18 576-0004, Japan

19

20 \* Corresponding author

21 Souta Nakajima: n.souta891@gmail.com

22 Watershed Restoration Team, Water Environment Research Group, Public Works Research Institute,  
23 Minamihara 1-6, Tsukuba, Ibaraki 305-8516, Japan

24 Phone: +81-29-879-6775, Fax: +81-29-869-5082

25

26 ORCID

27 Souta Nakajima: <https://orcid.org/0000-0003-3701-5428>

28 Shun K. Hirota: <https://orcid.org/0000-0002-6104-1119>

29 Yoshihisa Suyama: <https://orcid.org/0000-0002-3136-5489>

30 Futoshi Nakamura: <https://orcid.org/0000-0003-4351-2578>

31

## 32 **Acknowledgments**

33 We thank Nobuo Ishiyama for his cooperation in validating the hydrological model. This study is

34 partly supported by the research fund for the Ishikari and Tokachi Rivers provided by the Ministry of

35 Land, Infrastructure, Transport and Tourism of Japan.

36

37 **Abstract**

38 **Context:** Global climate change poses a significant threat to the habitat connectivity of cold-water-  
39 adapted organisms, leading to species extinctions. If gene flow can be modeled by landscape variables,  
40 changes in connectivity among populations could be predicted. However, in dendritic and  
41 heterogeneous stream ecosystems, few studies have estimated the changes in gene flow from genetic  
42 data, in part due to the difficulty in applying landscape genetics methods and accessing water  
43 temperature information.

44 **Objectives:** Inferring the determinants and future changes of the gene flow in the cold-water adapted  
45 fluvial sculpin *Cottus nozawae* using a recently developed model-based riverscape genetics technique  
46 and a hydrological model for estimating water temperature.

47 **Methods:** The strength of gene flow on each stream section was modeled by watershed-wide  
48 riverscape variables and genome-wide SNP data for *C. nozawae* in the upper reaches of the Sorachi  
49 River, Hokkaido, Japan. Future changes in gene flow were inferred by this model and hydrologically  
50 estimated water temperatures under the high greenhouse gas concentration scenario (IPCC RCP8.5).

51 **Results:** Stream order, water temperature, slope, and distance were selected as riverscape variables  
52 affecting the strength of gene flow in each stream section. In particular, the trend of greater gene flow  
53 in sections with higher stream order and lower temperature fluctuations or summer water temperatures  
54 was pronounced. The map from the model showed that gene flow is overall prevented in small  
55 tributaries in the southern area, where spring-fed environments are less prevalent. Estimating future  
56 changes, gene flow was predicted to decrease dramatically at the end of the 21st century.

57 **Conclusions:** Our results demonstrated that the connectivity of cold-water sculpin populations is  
58 expected to decline dramatically in a changing climate. Riverscape genetic modeling is useful for  
59 gaining information on population connectivity that does not fully coincide with habitat suitability.

60

61 **Keywords**

62 model-based riverscape genetics; cold-water fish; *Cottus*; water temperature; global warming

63

## 64 **Introduction**

65 Global climate change modifies water temperatures and flow regimes, the two key habitat factors  
66 affecting freshwater species, posing a critical threat to stream ecosystems (Barbarossa et al. 2021). The  
67 spatial distribution of species' suitable habitats shifts with environmental changes, and population  
68 fragmentation due to impassable environments may eventually result in local and/or species  
69 extinctions (Woodward et al. 2010). Numerous studies have predicted changes in species distributions  
70 and suitable habitats of stream organisms (Elith and Leathwick 2009; Comte et al. 2012; Ishiyama et  
71 al. 2023; Rahel et al. 1996), but how will the actual population connectivity and migration potential  
72 change?

73         Gene flow represents the functional connectivity among wild populations and is critical in  
74 species viability (Kottler et al. 2021; Manel and Holderegger 2013). The strength of gene flow is  
75 usually discussed individually from the observed genetic structure, but if gene flow could be modeled  
76 by landscape variables, the gained knowledge regarding gene flow could be generalized and used to  
77 predict its future changes (McRae and Beier 2007). The relationships between gene flow and  
78 landscape variables have been investigated in the field of landscape genetics (Balkenhol et al. 2015).  
79 However, most analytical techniques developed in landscape genetics exert only poor power in linear  
80 and dendritic stream ecosystems (Davis et al. 2018; Chafin et al. 2021), making it difficult to predict  
81 future changes in gene flow in riverscapes. Even in streams, regression models can be created by  
82 contrasting a genetic distance matrix against pairwise differences in local conditions (Grummer et al.  
83 2019), but this approach fails to account for the network architecture and for the attributes in all the  
84 spaces that individuals must pass through when traveling between sampling sites (Davis et al. 2018;  
85 White et al. 2020; Escalante et al. 2020). Another versatile approach to investigating the effects of  
86 landscape elements on gene flow is defining "landscape resistance" surfaces and assessing the  
87 relationship between genetic distance and cumulative resistance between populations (isolation by  
88 resistance; IBR (McRae 2006)). Although this idea has been applied to studies on stream ecosystems  
89 in several cases (e.g., Inoue and Berg 2017; Oliveira et al. 2019; Landguth et al. 2016; Escalante et al.  
90 2018), the landscape resistance must be parametrized *a priori* through expert opinion or other  
91 empirical methods (e.g., using the inverse of species distribution model estimates) (Spear et al. 2015;

92 Zeller et al. 2012). To understand the gene flow itself, its determinants should be identified directly  
93 from genetic data (Sartor et al. 2022; Wasserman et al. 2010). Fortunately, alternative methods for  
94 modeling gene flow from genetic data within a spatially explicit graph-theoretic framework have been  
95 developed rapidly in recent years (White et al. 2020; Chafin et al. 2021). Although not yet practically  
96 applied to predictions under environmental changes, we thought that these “riverscape genetics”-  
97 dedicated methods are the key to determining landscape resistance and modeling current and future  
98 gene flow.

99 Another theme that makes riverscape genetics challenging is the data availability of key  
100 environmental elements such as water temperatures. For terrestrial organisms, globally available  
101 climate data such as WorldClim (Hijmans et al. 2005) are commonly used to estimate the effects of  
102 climate change. However, data on current and future water temperatures that are critical for stream  
103 organisms are difficult to obtain as are data on flow rate. Although some studies have used air  
104 temperature data as a surrogate of water temperatures (Almodóvar et al. 2012), water temperatures do  
105 not actually coincide with air temperatures. In particular, local spatial heterogeneity in water  
106 temperatures caused by groundwater discharge and other factors is truly a source of ecosystem  
107 diversity and resilience to climate change that cannot be ignored (Koizumi and Maekawa 2004;  
108 Nakajima et al. 2021; Ishiyama et al. 2023; Nakamura 2022). Therefore, it is critical in riverscapes to  
109 utilize water temperature information considering the spatial heterogeneity generated by  
110 hydrogeological factors.

111 *Cottus nozawae* is a cold-water-adapted sculpin inhabiting northern Japan. Since the  
112 distribution and ecology of this species are highly influenced by summer water temperatures (Yagami  
113 and Goto 2000), available habitats are expected to decrease significantly under climate change (Suzuki  
114 et al. 2021). At a local scale, streams with low summer water temperatures characterized by spring-fed  
115 environments have been shown to display high population densities and to be the source of individuals  
116 in a watershed (Suzuki et al. 2021; Nakajima et al. 2021). Under ongoing climate change, the  
117 migration of this species is expected to be frequently blocked by unsuitable habitats, resulting in  
118 population fragmentation and shrinkage. To sustain the species into the future, it is critical to  
119 accurately predict the relationship between population connectivity and climate-related variables. Such

120 predictions will contribute to the advancement of climate change adaptation measures for this species,  
121 such as by identifying sections where stream continuity should be ensured.

122         Considering the challenges of data availability and analysis in riverscape genetics, we thought  
123 that the recently developed model-based riverscape genetics approaches and physics-based  
124 hydrological model to estimate water temperatures would enable the modeling and future prediction of  
125 gene flow in cold-water fish. The aims of this study are (i) to identify the factors determining the gene  
126 flow of *C. nozawae* in the stream network, (ii) to model the strength of gene flow using riverscape  
127 variables and predict its future changes, and (iii) to discuss the applicability of riverscape genetic  
128 modeling in conservation ecology.

129

## 130 **Material and Methods**

### 131 *Study sites and sampling*

132 In 2019, small pieces of fin tissue were sampled from 376 individuals of *C. nozawae* caught by  
133 electrofishing (model 12-B Backpack Electrofisher; Smith-Root Inc.) at 13 sites located in the  
134 upstream section of the Sorachi River, Hokkaido, Japan (Fig. 1; Table S1). Because no river-crossing  
135 structures that would obviously prevent fish migration are present between sampling sites, this area is  
136 considered suitable for evaluating the effects of riverscape variables. Regarding the environmental  
137 conditions, the tributaries in the northern volcanic watersheds have spring-fed environments with  
138 stable water temperatures and flow regimes (García Molinos et al. 2022; Ishiyama et al. 2023). For  
139 riverscape genetic modeling, the stream network among sampling sites was viewed as a graph  
140 consisting of 24 “nodes” and 23 “edges” (Fig. 2a). We defined “nodes” as the sampling sites and  
141 major tributary confluences between them, and analysis was conducted with “edges”, the stream  
142 segments between adjacent nodes, as units.

143

### 144 *Genetic data*

145         Genomic DNA was extracted using the QIAGEN DNeasy Blood and Tissue Kit (QIAGEN  
146 Inc.). In this study, we used the multiplexed ISSR genotyping by sequencing (MIG-seq) method  
147 (Suyama and Matsuki 2015; Suyama et al. 2022), a technique in which loci between two microsatellite

148 regions are amplified and neutral genome-wide single nucleotide polymorphisms (SNPs) are detected.  
149 A MIG-seq library preparation and read quality filtering were performed according to the protocol  
150 described in Suyama et al. (2022), with the modification that two runs were conducted and the  
151 obtained data were combined after quality filtering. In addition, quality filtering was performed on 71  
152 bases with six 5'-end bases and three 3'-end bases removed. After quality filtering, SNP selection was  
153 performed using STACKS 2.41 (Catchen et al. 2013). First, the reads were grouped to each locus  
154 using the *ustacks*, *cstacks*, *sstacks*, *tsv2bam*, and *gstacks* commands with the following parameters  
155 recommended by Paris et al. (2017): minimum depth option creating a stack ( $m$ ) = 3, maximum  
156 distance between stacks ( $M$ ) = 2, maximum mismatches between loci when building the catalog  
157 ( $n$ ) = 2, and number of mismatches allowed to align secondary reads ( $N$ ) = 4. From the derived dataset  
158 of assembled loci, SNPs were detected using the *populations* commands under the following criteria:  
159 only loci present at a rate of more than 80% of individuals within all populations were extracted (-p 13  
160 -r 0.8); the minimum minor allele frequency was 5% (--min-maf 0.05); sites showing excess  
161 heterozygosity were removed (--max-obs-het 0.6); and the output was limited to one SNP per locus (--  
162 write-single-snp). After filtering, 212 SNPs were obtained.

163 For populations in each sampling site, the expected heterozygosity ( $H_E$ ) and fixation index  
164 ( $F_{IS}$ ) were calculated using the *populations* command in STACKS. Significant deviations from Hardy–  
165 Weinberg equilibrium, as indicated by  $F_{IS}$  deviating from zero, were tested by 1000 randomizations  
166 using FSTAT 2.9.4 (Goudet 1995). Genetic differentiation among populations was assessed by  $G_{ST}$   
167 (Nei 1973) and  $D_{PS}$  (Bowcock et al. 1994).  $D_{PS}$  is the genetic distance based on the dissimilarities of  
168 population allele pools and reflects gene flow over a shorter timescale (approximately 10 generations;  
169 Landguth et al. 2010; Leroy et al. 2018), whereas  $G_{ST}$  is assumed to reflect long-term gene flow  
170 (Holsinger and Weir 2009).  $G_{ST}$  was calculated using GenAlEx 6.51 (Peakall and Smouse 2012), and  
171  $D_{PS}$  was calculated using the package graph4lg (Savary et al. 2021) in R 3.6.0 (R Core Team 2019).  
172 To understand the general patterns of population structure, STRUCTURE 2.3.4 (Pritchard et al. 2000)  
173 was performed in the setting of the admixture and allele frequency correlated model with previous  
174 sampling location information (LOCPRIOR; Hubisz et al. 2009). The algorithm was run 10 times for  
175 each K from 1 to 10 with a burn-in of 20,000 followed by 30,000 MCMC replicates. The program



176 CLUMPAK (Kopelman et al. 2015) was then used to summarize the results for each K. STRUCTURE  
177 HARVESTER (Earl and vonHoldt 2012) was employed to calculate the probability of the data for  
178 each K (LnP(D); Pritchard et al. 2000), the corresponding standard deviation, and the  $\Delta K$  (Evanno et  
179 al. 2005).

180

### 181 *Riverscape data*

182 Riverscape variables were collected as a unit of edges. Edge length, slope, stream orders, and  
183 catchment area were calculated in ArcGIS 10.7.1 (ESRI Inc.) using National Land Numerical  
184 Information (nlftp.mlit.go.jp) from the Ministry of Land, Infrastructure, Transport and Tourism  
185 (MLIT) of Japan. Flow rate and water temperature were estimated by a hydrological model based on  
186 Suzuki et al. (2022), which considers differences in groundwater discharge depending on catchment  
187 geology (see Appendix 1 for details). Briefly, the daily flow rate on the stream in each 1 km mesh was  
188 reproduced by four-layered tank models (Sugawara 1979), and the flow and heat flux were tracked  
189 along the streamflow. Importantly, different tank parameters were given for the volcanic areas and  
190 other areas, based on validation using measured water temperature data from field surveys at multiple  
191 sites in the study area. Flow rate and water temperature from September 2018 to August 2019 were  
192 reproduced and used to calculate the riverscape variables. In future predictions, 1 km-downscaled data  
193 on meteorological elements (Ueda et al. 2020), calculated under the climate data projected in the  
194 representative concentration pathway scenario 8.5 (RCP8.5) in the IPCC 5th Assessment (IPCC 2014),  
195 was used to derive the input water amount to the tank model. We used the mean of the predicted  
196 variables for the years 2081 to 2100 (all from September to next August) as future riverscape  
197 variables.

198

### 199 *Gene flow analysis*

200 We probabilistically modeled the relative migration rate (edge passability) of each edge as a function  
201 of riverscape variables using the “BGR model” (White et al. 2020). This is a novel method that can  
202 model bidirectional gene flow in stream networks using genetic distance matrices as input data and  
203 riverscape variables as explanatory variables, rigorously accounting for the spatial autocorrelation

204 structure of stream networks using a graph-theoretical framework and a spatial autoregressive model.  
205 Specifically, the nearly homogeneous stream segments (delimited by nodes that are sampling sites or  
206 major tributary confluences) were defined as edges, and the relative migration rate (edge passability;  
207  $w_{ij}$ ) of each edge linking nodes  $i$  and  $j$  was estimated as a function of  $k$  riverscape variables ( $x_{ij1}, x_{ij2},$   
208  $\dots, x_{ijk}$ ) and the corresponding parameters ( $\beta_1, \beta_2, \dots, \beta_k$ ) as:

$$209 \quad w_{ij} = \exp(\beta_0 + \sum_k \beta_k x_{ijk})$$

210 where  $\beta_0$  is the intercept term. Here, all riverscape variables were normalized from 0 to 1. The  
211 posterior distribution of parameters  $\beta_0, \beta_1, \dots, \beta_k$  was estimated by a Markov Chain Monte Carlo  
212 (MCMC) sampler, to fit the input genetic data. The mathematics linking  $w_{ij}$  to genetic distance are  
213 described in Peterson et al. (2019).

214 The BGR model was run in R. We used  $G_{ST}$  and  $D_{PS}$  as genetic distances and 10 possible  
215 riverscape variables (Table 1; Fig. S1) as covariates  $x_{ijk}$ . All variables except direction are symmetric.  
216 For each summary statistic, forward selections were conducted based on the deviance information  
217 criterion (DIC). Variables were added until the DIC no longer decreased by 7 or more (Cain and  
218 Zhang 2019). At each step of the forward selection, the variables that were highly correlated  
219 (Pearson's  $r > 0.7$ ) with other variables already included in the model were not added to the model.  
220 Models with fewer than four variables were run for 50,000 MCMC iterations and parameters were  
221 estimated after 25,000 burn-in. Models with four or more variables were run for 100,000 iterations  
222 including 50,000 burn-in. After the final model was identified, we conducted a long run with 500,000  
223 iterations including 200,000 burn-in, to accurately estimate the  $\beta$  values and 95% credible intervals.  
224 Landscape resistance, calculated as the inverse of  $w_{ij}$  of each edge, was estimated and mapped from  
225 the selected models. To evaluate the estimates, the correlations between genetic distances and  
226 estimated landscape resistance (sum of edges between populations) were calculated by Mantel tests  
227 with 9999 permutations, and compared to the correlations between genetic distances and waterway  
228 geographical distance. The Mantel tests were conducted using the package VEGAN 2.5.6 (Oksanen et  
229 al. 2019) in R. Future landscape resistance was inferred by substituting the future water temperature  
230 variable into the final BGR model. At this stage, we used the model derived from  $D_{PS}$  because  $G_{ST}$

231 displays long-term patterns and  $D_{PS}$  is more likely to reflect current changes in gene flow.

232

## 233 **Results**

234 The level of  $H_E$  was similar across the watershed (ranged from 0.241–0.272), and  $F_{IS}$  ranged from -  
235 0.012–0.023 with no populations deviating significantly from zero (Table S1). The average  $G_{ST}$  was  
236 0.029 (ranged from 0.000–0.047; Table S2) and  $D_{PS}$  was 0.087 (ranged from 0.050–0.135). In the  
237 STRUCTURE, while  $\ln P(D)$  for each  $K$  increased progressively,  $\Delta K$  was highest at  $K = 2$ , and locally  
238 maximum at  $K = 6$  (Fig. S2). Populations in the southern area were grouped into distinct clusters from  
239 low  $K$ , and as  $K$  increased, populations in other tributaries were also mixed with geographically  
240 uneven clusters. The strength of population structure differed geographically (Fig. 2a), but the factors  
241 determining this difference are not known by the STRUCTURE. From the forward selection of the  
242 model explaining the strength of gene flow, Shreve's stream order, water temperature fluctuation,  
243 slope, and edge length were selected for  $G_{ST}$ , and Strahler's stream order and summer water  
244 temperature were selected for  $D_{PS}$ , in this order (Tables 2 and S3). In both cases, the first and second  
245 variables added to the model were the stream order and water temperature, respectively. While  
246 different types of variables were selected for  $G_{ST}$  and  $D_{PS}$  (Shreve's or Strahler's; summer water  
247 temperature or water temperature fluctuation), these results show the importance of the stream order  
248 and water temperature on the strength of gene flow. The stream orders had a positive effect on gene  
249 flow, while the water temperature fluctuation or summer water temperature had a negative effect. The  
250 effect ( $\beta$ ) of the water temperature on gene flow was higher in  $D_{PS}$  than in  $G_{ST}$ . In  $G_{ST}$ , the slope and  
251 edge length were also selected and had negative effects, indicating their relevance to long-term gene  
252 flow. Geographically, the southern upstream area had generally higher landscape resistance (lower  
253 gene flow) than the main stream, while in the northern volcanic area, landscape resistance was not so  
254 high even upstream (Fig. 2). The Mantel tests between the genetic distances and estimated landscape  
255 resistance suggested significant relationships ( $r = 0.46$ ,  $p < 0.05$  for  $G_{ST}$ ;  $r = 0.60$ ,  $p < 0.01$  for  $D_{PS}$ ),  
256 and the correlations were much higher than those between the genetic and geographic distances (Fig.  
257 3). The future prediction indicated that the landscape resistance would increase overall from the  
258 current levels. Some sections in the main stream and in the upper reaches in the volcanic area were

259 estimated to exhibit as high landscape resistance levels as the present southern upstream area. The  
260 southern upstream area was projected to display very high resistance.

261

## 262 **Discussion**

263 In this study, we succeeded in modeling and future predicting of gene flow of *C. nozawae* in the  
264 stream network. Although there are still challenges in the modeling technique (e.g., simplicity of  
265 model assumptions, difficulty of model evaluation, etc.), the modeled landscape resistance explained  
266 the genetic distances well (Fig. 3); the strength of gene flow could be largely explained by riverscape  
267 variables.

268 It was a somewhat unexpected result that the stream order was identified as the variable with  
269 the strongest effect on gene flow. Previous studies of cold-water fish have reported both higher and  
270 lower gene flow in streams with higher stream orders (Aunins et al. 2015; Escalante et al. 2018; White  
271 et al. 2020). Within the arbitrary study areas, main streams tend to have higher water temperatures and  
272 are often unsuitable environments for cold-water fish. On the other hand, in dendritic stream  
273 structures, confluences are often known to be stable gene accumulation and source points for stream  
274 organisms (Grant et al. 2007; Paz-Vinas and Blanchet 2015), and the downstream passage of those  
275 organisms may result in higher gene flow in higher-order streams. In addition, as the main stream  
276 tends to be more severely affected by flooding (Han et al. 2007; Koizumi et al. 2013), individuals,  
277 especially those of low-mobility species, may have a greater chance of being flushed. There may be  
278 differences regarding which processes are predominant depending on the studied species or areas.  
279 Summer water temperature (or water temperature fluctuation in  $G_{ST}$ ) negatively affected gene flow.  
280 This is probably because streams with high summer water temperatures and large fluctuations are not  
281 suitable environments for *C. nozawae* (Suzuki et al. 2021), making successful dispersal difficult.  
282 While it is not uncommon for studies of cold-water fishes to implicate an association between gene  
283 flow and water temperature-related variables (Kanno et al. 2011; Escalante et al. 2018; Hand et al.  
284 2016), the present study was able to represent this pattern using more realistic water temperature  
285 information. The model from  $G_{ST}$  also included the slope and edge length, but the model from  $D_{PS}$  did  
286 not. We found that topography and distance affected the formation of the long-term population

287 structure as in many other systems (Kanno et al. 2011; Caldera and Bolnick 2008), but that most of the  
288 current gene flow can be explained by the stream order and water temperature. The upstream-  
289 downstream direction did not affect gene flow, probably because environmental conditions influence  
290 the direction of gene flow (Nakajima et al. 2021).

291 Maps displaying modeled landscape resistance from  $G_{ST}$  and  $D_{PS}$  were visually similar (Fig.  
292 2), indicating that the pattern has probably been maintained for a long time. Overall, gene flow is  
293 prevented in small tributaries in the southern area. This area displays higher water temperature  
294 fluctuations than the northern volcanic area where spring-fed environments are more prevalent  
295 (Ishiyama et al. 2023); gene flow in the southern area is probably suppressed by the effects of water  
296 temperature. When comparing this geographical pattern with the STRUCTURE barplots, the upper  
297 reaches in the non-volcanic area where gene flow is prevented roughly corresponded to the areas  
298 where a strong population structure was observed. While the reason for the heterogeneity in the  
299 strength of population structure could not be known by the STRUCTURE, a possible explanation was  
300 explicitly presented in the gene flow analysis.

301 Under the RCP8.5 scenario, reduced gene flow and increased landscape resistance across the  
302 watershed were predicted (Fig. 2d). Since the studied species exhibited a clear genetic structure only  
303 in the southern area, the prediction that the northern area will have the same level of gene flow as the  
304 present southern area indicates that each tributary within the watershed may experience genetic  
305 fragmentation in the future. Nevertheless, gene flow in the northern area was expected to be  
306 maintained spatially continuously to some extent, indicating that streams with volcanic watersheds are  
307 important for ensuring population connectivity under climate change. A previous study suggested that  
308 streams with low summer temperatures behave as source habitats in the watershed (Nakajima et al.  
309 2021). Our study showed that these streams may serve not only as source habitats but also as  
310 migration pathways in the watershed. As a scenario analysis, Inoue and Berg (2017) considered  
311 landscape resistance to be the inverse of the species distribution model (SDM) estimates and predicted  
312 that an increased landscape resistance would reduce the gene flow of freshwater bivalves in the future.  
313 This is a valuable study that attempts to predict future changes in gene flow; however, it is known that  
314 the habitat suitability maps created by SDMs provide poor estimates of genetic resistance, because of

315 the conceptual differences between habitat selection and entire gene flow (Wasserman et al. 2010,  
316 2012; Sator et al. 2022; Mateo-Sánchez 2015). Actually, in *C. nozawae*, the SDM created in Suzuki et  
317 al. (2021) indicated that the catchment area, analogous to the stream order, had a negative effect on the  
318 occurrence of this species, in contrast to the gene flow characteristics estimated in our study.  
319 Therefore, genetic population connectivity should be considered separately from habitat suitability.

320 The present study is novel in that gene flow was modeled using riverscape variables identified  
321 from genetic data and including water temperature. Our results showed that gene flow in the cold-  
322 water sculpin is expected to decrease dramatically in response to a changing climate. Therefore, under  
323 ongoing climate change, it is important to maintain habitat continuity within the distribution ranges. In  
324 particular, it is necessary to consider that the risk is high in sections where water temperature  
325 fluctuations are large (such as non-volcanic watersheds). Additionally, while main streams may be less  
326 suitable as habitats, they are important as migration corridors. No structures such as weirs should be  
327 installed so that drifted individuals can quickly enter suitable habitats.

328 To obtain more robust results, it would be desirable to increase the number of sampling  
329 populations. This study has the potential for further development. For example, demography  
330 simulations using inferred landscape resistance (Landguth et al. 2010, 2016) could reveal population  
331 viability. Also, combined with habitat quality analyses such as SDMs, population connectivity could  
332 be quantified for more detailed predictions from the viewpoint of habitat availability (Saura and  
333 Pascual-Hortal 2007). We hope that riverscape genetic modeling will be applied to predict the  
334 consequences of environmental changes on a variety of freshwater organisms.

335

## 336 **References**

- 337 Almodóvar A, Nicola GG, Ayllón D, Elvira B (2012) Global warming threatens the persistence of  
338 Mediterranean brown trout. *Glob Chang Biol* 18:1549–1560. [https://doi.org/10.1111/j.1365-  
339 2486.2011.02608.x](https://doi.org/10.1111/j.1365-2486.2011.02608.x)
- 340 Aunins AW, Petty JT, King TL et al (2015) River mainstem thermal regimes influence population  
341 structuring within an appalachian brook trout population. *Conserv Genet* 16:15–29.  
342 <https://doi.org/10.1007/s10592-014-0636-6>

343 Balkenhol N, Cushman SA, Storfer A, Waits LP (2015) Introduction to landscape genetics - concepts,  
344 methods, applications. In: Balkenhol N, Cushman SA, Storfer A, Waits LP (ed) Landscape  
345 Genetics. Wiley, New York, pp 1–8

346 Barbarossa V, Bosmans J, Wanders N, et al (2021) Threats of global warming to the world’s  
347 freshwater fishes. Nat Commun 12:1701. <https://doi.org/10.1038/s41467-021-21655-w>

348 Bowcock AM, Ruiz-Linares A, Tomfohrde J, et al (1994) High resolution of human evolutionary trees  
349 with polymorphic microsatellites. Nature 368:455–457. <https://doi.org/10.1038/368455a0>

350 Cain MK, Zhang Z (2019) Fit for a Bayesian: An evaluation of PPP and DIC for structural equation  
351 modeling. Struct Equ Model 26:39–50. <https://doi.org/10.1080/10705511.2018.1490648>

352 Caldera EJ, Bolnick DI (2008) Effects of colonization history and landscape structure on genetic  
353 variation within and among threespine stickleback (*Gasterosteus aculeatus*) populations in a  
354 single watershed. Evol Ecol Res 10:575–598

355 Catchen J, Hohenlohe PA, Bassham S, et al (2013) Stacks: An analysis tool set for population  
356 genomics. Mol Ecol 22:3124–3140. <https://doi.org/10.1111/mec.12354>

357 Chafin TK, Mussmann SM, Douglas MR, Douglas ME (2021) Quantifying isolation-by-resistance and  
358 connectivity in dendritic ecological networks. bioRxiv.  
359 <https://doi.org/10.1101/2021.03.25.437078>

360 Comte L, Buisson L, Daufresne M, Grenouillet G (2012) Climate-induced changes in the distribution  
361 of freshwater fish: observed and predicted trends. Freshw Biol 58:625–639.  
362 <https://doi.org/10.1111/fwb.12081>

363 Davis CD, Epps CW, Flitcroft RL, Banks MA (2018) Refining and defining riverscape genetics: How  
364 rivers influence population genetic structure. WIREs Water 5:e1269.  
365 <https://doi.org/10.1002/wat2.1269>

366 Earl DA, vonHoldt BM (2012) STRUCTURE HARVESTER: A website and program for visualizing  
367 STRUCTURE output and implementing the Evanno method. Conserv Genet Resour 4:359–361.  
368 <https://doi.org/10.1007/s12686-011-9548-7>

369 Elith J, Leathwick JR (2009) Species distribution models: Ecological explanation and prediction  
370 across space and time. Annu Rev Ecol Evol Syst 40:677–697.

371 <https://doi.org/10.1146/annurev.ecolsys.110308.120159>

372 Escalante MA, García-De León FJ, Ruiz-Luna A et al (2018) The interplay of riverscape features and  
373 exotic introgression on the genetic structure of the Mexican golden trout (*Oncorhynchus*  
374 *chrysogaster*), a simulation approach. *J Biogeogr* 45:1500–1514.  
375 <https://doi.org/10.1111/jbi.13246>

376 Escalante MA, Perrier C, García-De León FJ et al (2020) Genotyping-by-sequencing reveals the  
377 effects of riverscape, climate and interspecific introgression on the genetic diversity and local  
378 adaptation of the endangered Mexican golden trout (*Oncorhynchus chrysogaster*). *Conserv*  
379 *Genet* 21:907–926. <https://doi.org/10.1007/s10592-020-01297-z>

380 Evanno G, Regnaut S, Goudet J (2005) Detecting the number of clusters of individuals using the  
381 software STRUCTURE: A simulation study. *Mol Ecol* 14:2611–2620.  
382 <https://doi.org/10.1111/j.1365-294X.2005.02553.x>

383 García Molinos J, Ishiyama N, Sueyoshi M, Nakamura F (2022) Timescale mediates the effects of  
384 environmental controls on water temperature in mid- to low-order streams. *Sci Rep* 12:12248.  
385 <https://doi.org/10.1038/s41598-022-16318-9>

386 Goudet J (1995) FSTAT (Version 1.2): a computer program to calculate F-statistics. *J Hered* 86:485–  
387 486. <https://doi.org/10.1093%2Foxfordjournals.jhered.a111627>

388 Grant EHC, Lowe WH, Fagan WF (2007) Living in the branches: population dynamics and ecological  
389 processes in dendritic networks. *Ecol Lett* 10:165–175. [https://doi.org/10.1111/j.1461-](https://doi.org/10.1111/j.1461-0248.2006.01007.x)  
390 [0248.2006.01007.x](https://doi.org/10.1111/j.1461-0248.2006.01007.x)

391 Grummer JA, Beheregaray LB, Bernatchez L (2019) Aquatic landscape genomics and environmental  
392 effects on genetic variation. *Trends Ecol Evol* 34:641–654.  
393 <https://doi.org/10.1016/j.tree.2019.02.013>

394 Han CC, Tew KS, Fang LS (2007) Spatial and temporal variations of two cyprinids in a subtropical  
395 mountain reserve – a result of habitat disturbance. *Ecol Freshw Fish* 16:395–403.  
396 <https://doi.org/10.1111/j.1600-0633.2007.00227.x>

397 Hand BK, Muhlfeld CC, Wade AA et al (2016) Climate variables explain neutral and adaptive  
398 variation within salmonid metapopulations: the importance of replication in landscape genetics.



399 Mol Ecol 25:689–705. <https://doi.org/10.1111/mec.13517>

400 Hijmans RJ, Cameron SE, Parra JL, et al (2005) Very high resolution interpolated climate surfaces for  
401 global land areas. *Int J Climatol* 25:1965–1978. <https://doi.org/10.1002/joc.1276>

402 Holsinger KE, Weir BS (2009) Genetics in geographically structured populations: Defining,  
403 estimating and interpreting  $F_{ST}$ . *Nat Rev Genet* 10:639–650. <https://doi.org/10.1038/nrg2611>

404 Hubisz MJ, Falush D, Stephens M, Pritchard JK (2009) Inferring weak population structure with the  
405 assistance of sample group information. *Mol Ecol Resour* 9:1322–1332.  
406 <https://doi.org/10.1111/j.1755-0998.2009.02591.x>

407 Inoue K, Berg DJ (2017) Predicting the effects of climate change on population connectivity and  
408 genetic diversity of an imperiled freshwater mussel, *Cumberlandia monodonta* (Bivalvia:  
409 Margaritiferidae), in riverine systems. *Glob Chang Biol* 23:94–107.  
410 <https://doi.org/10.1111/gcb.13369>

411 IPCC (2014) Summary for policymakers. <https://www.ipcc.ch/report/ar5/wg2/>

412 Ishiyama N, Sueyoshi M, García Molinos J, et al (2023) Underlying geology and climate interactively  
413 shape climate change refugia in mountain streams. *Ecol Monogr*.  
414 <https://doi.org/10.1002/ecm.1566>

415 Kanno Y, Vokoun JC, Letcher BH (2011) Fine-scale population structure and riverscape genetics of  
416 brook trout (*Salvelinus fontinalis*) distributed continuously along headwater channel networks.  
417 *Mol Ecol* 20:3711–3729. <https://doi.org/10.1111/j.1365-294X.2011.05210.x>

418 Koizumi I, Kanazawa Y, Tanaka Y (2013) The fishermen were right: experimental evidence for  
419 tributary refuge hypothesis during floods. *Zool Sci* 30:375–379.  
420 <https://doi.org/10.2108/zsj.30.375>

421 Koizumi I, Maekawa K (2004) Metapopulation structure of stream-dwelling Dolly Varden charr  
422 inferred from patterns of occurrence in the Sorachi River basin, Hokkaido, Japan. *Freshw Biol*  
423 49:973–981. <https://doi.org/10.1111/j.1365-2427.2004.01240.x>

424 Kopelman NM, Mayzel J, Jakobsson M, et al (2015) Clumpak: A program for identifying clustering  
425 modes and packaging population structure inferences across K. *Mol Ecol Resour* 15:1179–1191.  
426 <https://doi.org/10.1111/1755-0998.12387>

427 Kottler EJ, Dickman EE, Sexton JP, et al (2021) Draining the swamping hypothesis: little evidence  
428 that gene flow reduces fitness at range edges. *Trends Ecol Evol* 36:533–544.  
429 <https://doi.org/10.1016/j.tree.2021.02.004>

430 Lamphere BA, Blum MJ (2012) Genetic estimates of population structure and dispersal in a benthic  
431 stream fish. *Ecol Freshw Fish* 21:75–86. <https://doi.org/10.1111/j.1600-0633.2011.00525.x>

432 Landguth EL, Bearlin A, Day CC, Dunham J (2016) CDMetaPOP: an individual-based, eco-  
433 evolutionary model for spatially explicit simulation of landscape demogenetics. *Methods Ecol*  
434 *Evol* 8:4–11. <https://doi.org/10.1111/2041-210X.12608>

435 Landguth EL, Cushman SA, Schwartz MK, et al (2010) Quantifying the lag time to detect barriers in  
436 landscape genetics. *Mol Ecol* 19:4179–4191. <https://doi.org/10.1111/j.1365-294X.2010.04808.x>

437 Leroy G, Carroll EL, Bruford MW et al (2018) Next-generation metrics for monitoring genetic erosion  
438 within populations of conservation concern. *Evol Appl* 11:1066–1083.  
439 <https://doi.org/10.1111/eva.12564>

440 Manel A, Holderegger R (2013) Ten years of landscape genetics. *Trends Ecol Evol* 28:614–621.  
441 <https://doi.org/10.1016/j.tree.2013.05.012>

442 Mateo-Sánchez MC, Balkenhol N, Cushman S, et al (2015) A comparative framework to infer  
443 landscape effects on population genetic structure: are habitat suitability models effective in  
444 explaining gene flow? *Landsc Ecol* 30:1405–1420. <https://doi.org/10.1007/s10980-015-0194-4>

445 McRae BH (2006) Isolation By Resistance. *Evolution* 60:1551–1561. <https://doi.org/10.1554/05-321.1>

446 McRae BH, Beier P (2007) Circuit theory predicts gene flow in plant and animal populations. *Proc*  
447 *Natl Acad Sci U S A* 104:19885–19890. <https://doi.org/10.1073/pnas.0706568104>

448 Nagasaka A, Sugiyama S (2010) Factors affecting the summer maximum stream temperature of small  
449 streams in northern Japan. *Bull Hokkaido For Res Inst* 47:35–43. (In Japanese with English  
450 abstract)

451 Nakajima S, Sueyoshi M, Hirota SK, et al (2021) A strategic sampling design revealed the local  
452 genetic structure of cold-water fluvial sculpin: a focus on groundwater-dependent water  
453 temperature heterogeneity. *Heredity* 127:413–422. <https://doi.org/10.1038/s41437-021-00468-z>

454 Nakamura F (2022) Riparian forests and climate change: interactive zone of green and blue

455 infrastructure. In: Nakamura F (ed) Green Infrastructure and Climate Change Adaptation.  
456 Springer, Singapore, pp 73–91

457 Nei M (1973) Analysis of gene diversity in subdivided populations. *Proc Natl Acad Sci U S A*  
458 70:3321–3323. <https://doi.org/10.1073/pnas.70.12.3321>

459 Oksanen JF, Blanchet G, Friendly M et al (2019) vegan: community ecology package. R package  
460 version 2.5-6. <https://CRAN.R-project.org/package=vegan>

461 Oliveira J dos A, Farias IP, Costa GC, Werneck FP (2019) Model-based riverscape genetics:  
462 disentangling the roles of local and connectivity factors in shaping spatial genetic patterns of two  
463 Amazonian turtles with different dispersal abilities. *Evol Ecol* 33:273–298.  
464 <https://doi.org/10.1007/s10682-019-09973-4>

465 Paris JR, Stevens JR, Catchen JM (2017) Lost in parameter space: a road map for stacks. *Methods*  
466 *Ecol Evol* 8:1360–1373. <https://doi.org/10.1111/2041-210X.12775>

467 Paz-Vinas I, Blanchet S (2015) Dendritic connectivity shapes spatial patterns of genetic diversity: A  
468 simulation-based study. *J Evol Biol* 28:986–994. <https://doi.org/10.1111/jeb.12626>

469 Peakall R, Smouse PE (2012) GenAlEx 6.5: Genetic analysis in Excel. Population genetic software for  
470 teaching and research-an update. *Bioinformatics* 28:2537–2539.  
471 <https://doi.org/10.1093/bioinformatics/bts460>

472 Peterson EE, Hanks EM, Hooten MB, et al (2019) Spatially structured statistical network models for  
473 landscape genetics. *Ecol Monogr* 89:e01355. <https://doi.org/10.1002/ecm.1355>

474 Pritchard JK, Stephens M, Donnelly P (2000) Inference of population structure using multilocus  
475 genotype data. *Genetics* 155:945–959. <https://doi.org/10.1093/genetics/155.2.945>

476 Rahel FJ, Keleher CJ, Anderson JL (1996) Potential habitat loss and population fragmentation for cold  
477 water fish in the North Platte River drainage of the Rocky Mountains: Response to climate  
478 warming. *Limnol Oceanogr* 41:1116–1123. <https://doi.org/10.4319/lo.1996.41.5.1116>

479 R Core Team (2019) R: a language and environment for statistical computing. R Foundation for  
480 Statistical Computing, Vienna, Austria. <https://www.R-project.org/>

481 Sartor CC, Wan HY, Pereira JA, et al (2022) Landscape genetics outperforms habitat suitability in  
482 predicting landscape resistance for congeneric cat species. *J Biogeogr* 49:2206–2217.

483 <https://doi.org/10.1111/jbi.14498>

484 Saura S, Pascual-Hortal L (2007) A new habitat availability index to integrate connectivity in  
485 landscape conservation planning: Comparison with existing indices and application to a case  
486 study. *Landsc Urban Plan* 83:91–103. <https://doi.org/10.1016/j.landurbplan.2007.03.005>

487 Savary P, Foltête JC, Moal H, et al (2021) graph4lg: A package for constructing and analysing graphs  
488 for landscape genetics in R. *Methods Ecol Evol* 12:539–547. [https://doi.org/10.1111/2041-](https://doi.org/10.1111/2041-210X.13530)  
489 [210X.13530](https://doi.org/10.1111/2041-210X.13530)

490 Spear SF, Cushman SA, McRae BH (2015) Resistance Surface Modeling in Landscape Genetics. In:  
491 Balkenhol N, Cushman SA, Storfer A, Waits LP (ed) *Landscape Genetics*. Wiley, New York, pp  
492 129–148

493 Sugawara M (1979) Automatic calibration of the tank model. *Hydrological Sciences Bulletin* 24:375–  
494 388. <https://doi.org/10.1080/02626667909491876>

495 Suyama Y, Hirota SK, Matsuo A, et al (2022) Complementary combination of multiplex high-  
496 throughput DNA sequencing for molecular phylogeny. *Ecol Res* 37:171–181.  
497 <https://doi.org/10.1111/1440-1703.12270>

498 Suyama Y, Matsuki Y (2015) MIG-seq: An effective PCR-based method for genome-wide single-  
499 nucleotide polymorphism genotyping using the next-generation sequencing platform. *Sci Rep*  
500 5:16963. <https://doi.org/10.1038/srep16963>

501 Suzuki H, Nakatsugawa M, Ishiyama N (2022) Climate change impacts on stream water temperatures  
502 in the snowy cold region according to geological conditions. *Water* 14:2166.  
503 <https://doi.org/10.3390/w14142166>

504 Suzuki K, Ishiyama N, Koizumi I, Nakamura F (2021) Combined effects of summer water  
505 temperature and current velocity on the distribution of a cold-water-adapted sculpin (*Cottus*  
506 *nozawae*). *Water* 13:975. <https://doi.org/10.3390/w13070975>

507 Ueda S, Nakatsugawa M, Usutani T (2020) Estimation of high-resolution downscaled climate  
508 information based on verification of water balance in watershed of Hokkaido. *Journal of Japan*  
509 *Society of Civil Engineers, Ser. B1 (Hydraulic Engineering)* 76:I\_25–I\_30.  
510 [https://doi.org/10.2208/jscejhe.76.2\\_I\\_25](https://doi.org/10.2208/jscejhe.76.2_I_25). (In Japanese with English abstract)

511 Wasserman TN, Cushman SA, Schwartz MK, Wallin DO (2010) Spatial scaling and multi-model  
512 inference in landscape genetics: *Martes americana* in northern Idaho. *Landsc Ecol* 25:1601–  
513 1612. <https://doi.org/10.1007/s10980-010-9525-7>

514 Wasserman TN, Cushman SA, Shirk AS, et al (2012) Simulating the effects of climate change on  
515 population connectivity of American marten (*Martes americana*) in the northern Rocky  
516 Mountains, USA. *Landsc Ecol* 27:211–225. <https://doi.org/10.1007/s10980-011-9653-8>

517 White SL, Hanks EM, Wagner T (2020) A novel quantitative framework for riverscape genetics. *Ecol*  
518 *Appl* 30:e02147. <https://doi.org/10.1002/eap.2147>

519 Woodward G, Perkins DM, Brown LE (2010) Climate change and freshwater ecosystems: Impacts  
520 across multiple levels of organization. *Philos Trans R Soc B Biol Sci* 365:2093–2106.  
521 <https://doi.org/10.1098/rstb.2010.0055>

522 Wright S (1943) Isolation by distance. *Genetics* 28:114–138. <https://doi.org/10.1093/genetics/28.2.114>

523 Yagami T, Goto A (2000) Patchy distribution of a fluvial sculpin, *Cottus nozawae*, in the Gakko River  
524 system at the southern margin of its native range. *Ichthyol Res* 47:277–286

525 Zeller KA, McGarigal K, Whiteley AR (2012) Estimating landscape resistance to movement: a  
526 review. *Landsc Ecol* 27:777–797. <https://doi.org/10.1007/s10980-012-9737-0>

527

## 528 **Statements & Declarations**

529 **Funding:** This study is partly supported by the research fund for the Ishikari and Tokachi Rivers  
530 provided by the Ministry of Land, Infrastructure, Transport and Tourism of Japan.

531 **Competing Interests:** The authors declare no competing interests.

532 **Author Contributions:** Conceptualization, S.N. and F.N.; Data curation, S.N. and S.K.H.; Formal  
533 analysis, S.N.; Funding acquisition; F.N.; Investigation, S.N., H.S., A.M., and S.K.H. ; Methodology,  
534 S.N., H.S., M.N., and Y.S.; Project administration, F.N.; Resources, S.N., M.N., A.M., and Y.S.;  
535 Software, S.N. and H.S., A.M., and S.K.H.; Supervision, M.N., Y.S. and F.N.; Validation, S.N. and  
536 F.N.; Visualization, S.N.; Writing – original draft, S.N. and H.S. ; Writing – review & editing, S.N.,  
537 H.S., M.N., A.M., S.K.H., Y.S., and F.N.

538 **Data Availability:** Genetic and environmental data generated in this study were deposited at Figshare

539 (doi: 10.6084/m9.figshare.19694989).

540

541 **Table 1** Riverscape variables considered in the present study.

Variable	Description	Hypothesis / Ecological importance	Ranges
Summer water temperature <sup>A</sup>	Mean water temperature from July to August (July 2019 to August 2019) [°C]	Streams with low summer water temperatures are suitable for <i>C. nozawae</i> occupancy/survival (Yagami and Goto 2000; Suzuki et al. 2021) and therefore migration may also occur frequently in these streams.	8.32–14.2
Water temperature fluctuation <sup>A</sup>	Standard deviation of the water temperature in one year (September 2018 to August 2019)	Thermally stable streams can be suitable for migration.	1.97–5.09
Drought water discharge <sup>BC</sup>	Flow rate on the day when the flow is 355th highest in one year [m <sup>3</sup> /s] (September 2018 to August 2019)	Drought water discharges, which particularly reflect the environmental heterogeneity created by groundwater (Nagasaka and Sugiyama 2010), ensure opportunities to colonize throughout the year.	0.07–6.24
Flow fluctuation <sup>AB</sup>	Coefficient of variation in the daily flow rate in one year (September 2018 to August 2019)	Hydrologically stable streams can be suitable for migration.	0.31–0.65
Edge length	Length of edges [km]	Isolation by distance (Wright 1943)	0.05–7.19
Slope	Mean gradient of the edge, i.e., the elevation range divided by edge length	Fish movement and migration are often impeded on steep slopes (Kanno et al. 2011).	4.15–56.5
Strahler's stream order <sup>C</sup>	Strahler's stream order of the edge	Even in cold-water fish, the mainstem may function as a corridor that facilitates connectivity among populations (White et al. 2020).	1–4
Shreve's stream order <sup>BC</sup>	Shreve's stream order (link magnitude), i.e., the numbers of confluence points upstream, at the midpoint of the edge	Given the dendritic arrangement and asymmetry of stream networks, sections with more confluence points upstream may increase the number of migrants passing through (Paz-Vinas and Blanchet 2015).	1–62
Catchment area <sup>BC</sup>	Cumulative area of the catchment calculated at the midpoint of the edge [km <sup>2</sup> ]	Sections with larger catchment areas may have more migrants passing through, based on the same principle as that of the stream order. Or, conversely, streams with larger catchment areas have been identified to have lower <i>C. nozawae</i> occupancies (Suzuki et al. 2021) and therefore it is also possible that less migration occurs in sections with larger catchment areas.	6.4–296.3
Direction	Whether the gene flow is toward the upstream (0) or downstream (1) direction	Most stream organisms have higher migration rates in the downstream direction than in the upstream direction (Lamphere and Blum 2012).	0 or 1

542 Variables with the same letters (A, B, C) have high correlations ( $|r| > 0.7$ ); these variables were not included in the same model.

543 **Table 2** Selected models explaining the strength of gene flow on the edges. Estimated  $\beta$  values  
 544 (median) and their 95% credible intervals (95% CI) are displayed.

Variables	$\beta$	95% CI
<b>(A) <math>G_{ST}</math></b>		
(Intercept)	5.84	5.65, 5.98
Shreve's stream order	4.51	3.96, 5.19
Water temperature fluctuation	-0.48	-0.61, -0.35
Slope	-0.94	-1.15, -0.67
Edge length	-0.42	-0.54, -0.32
<b>(B) <math>D_{PS}</math></b>		
(Intercept)	6.06	4.94, 6.85
Strahler's stream order	2.50	1.72, 3.15
Summer water temperature	-1.42	-2.49, -0.38

545

546 **Figure Legends**

547 **Fig. 1** Location of the study area. The blue network indicates the rivers belonging to the Ishikari River  
 548 system, which has the second largest watershed in Japan and includes the Sorachi River.

549

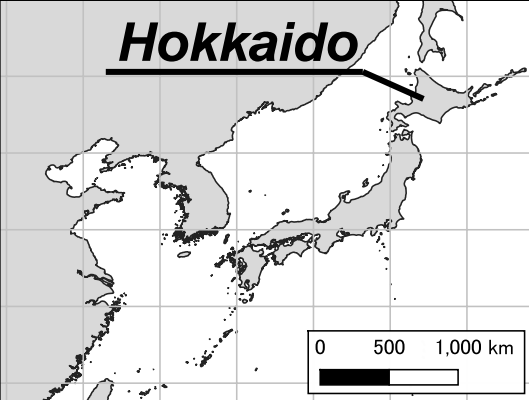
550 **Fig. 2** Maps of the Sorachi River watershed showing the study area (a) and landscape resistance  
 551 estimated by BGR models (b–d). In panel (a), sampling nodes (sampling sites) and unsampled nodes  
 552 (major confluences between them), which are delimitations of edges (stream sections), are denoted.  
 553 Barplots with each sampling node indicate the population structure inferred by STRUCTURE ( $K = 6$ ).  
 554 Landscape resistance is shown in three patterns: long-term gene flow modeled by  $G_{ST}$  (b), recent gene  
 555 flow modeled by  $D_{PS}$  (c), predicted gene flow at the end of the 21st century derived by substituting  
 556 future water temperatures into the model derived by  $D_{PS}$  (d).

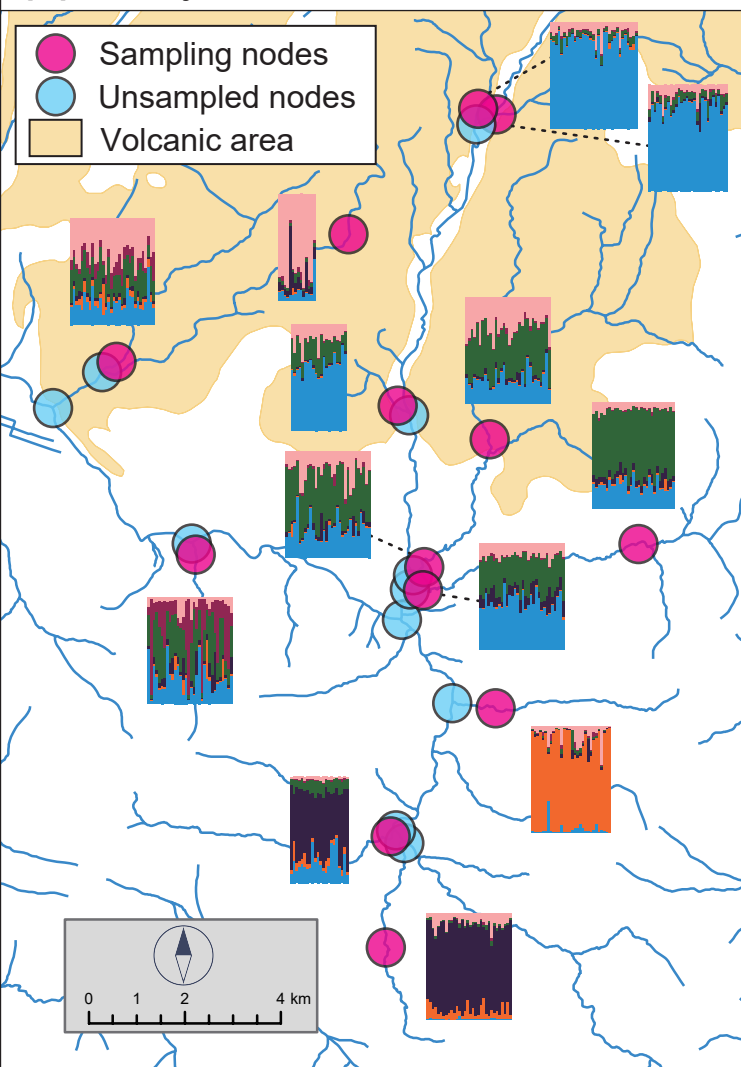
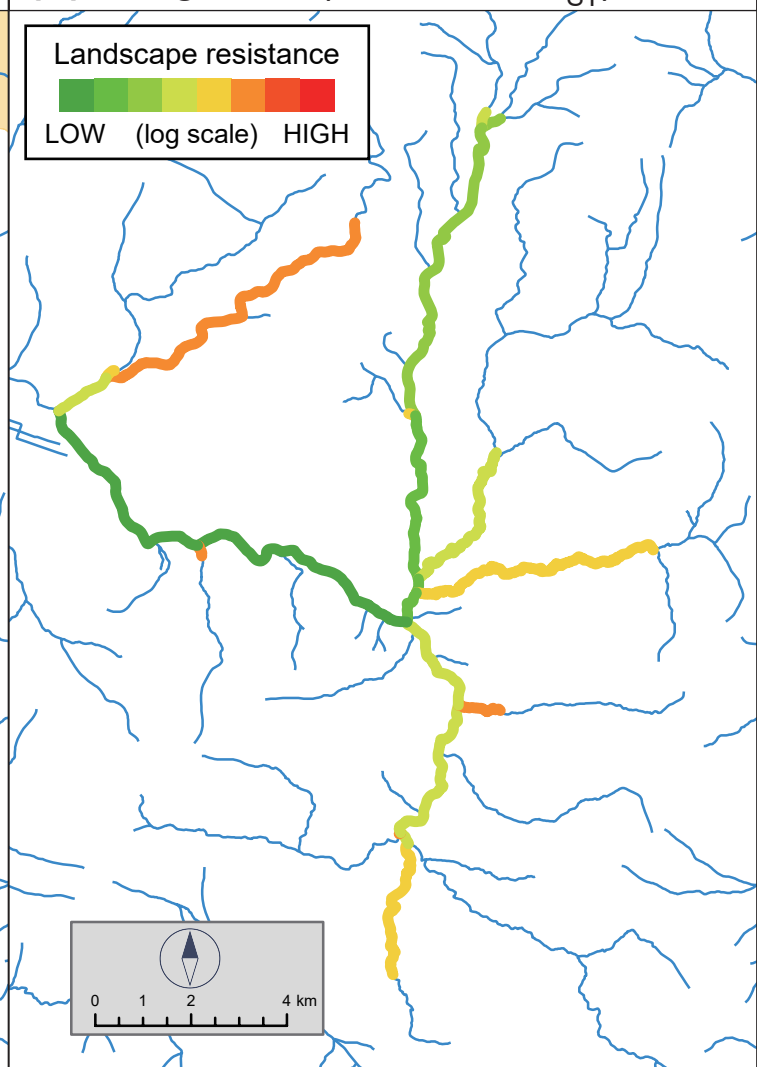
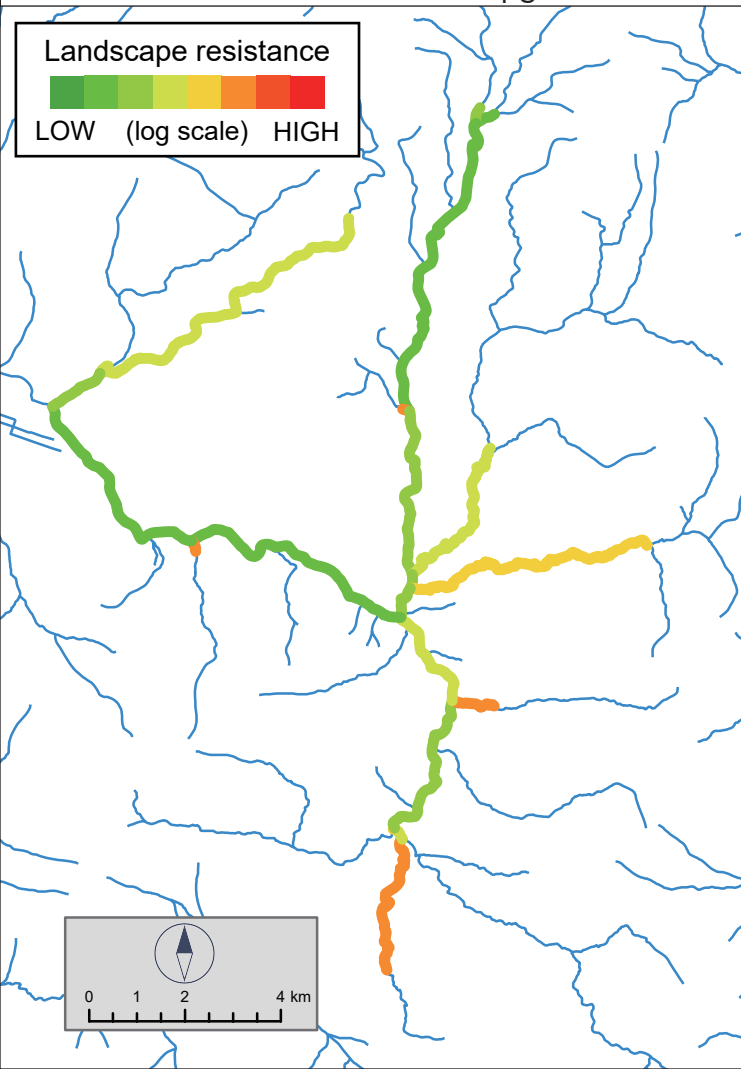
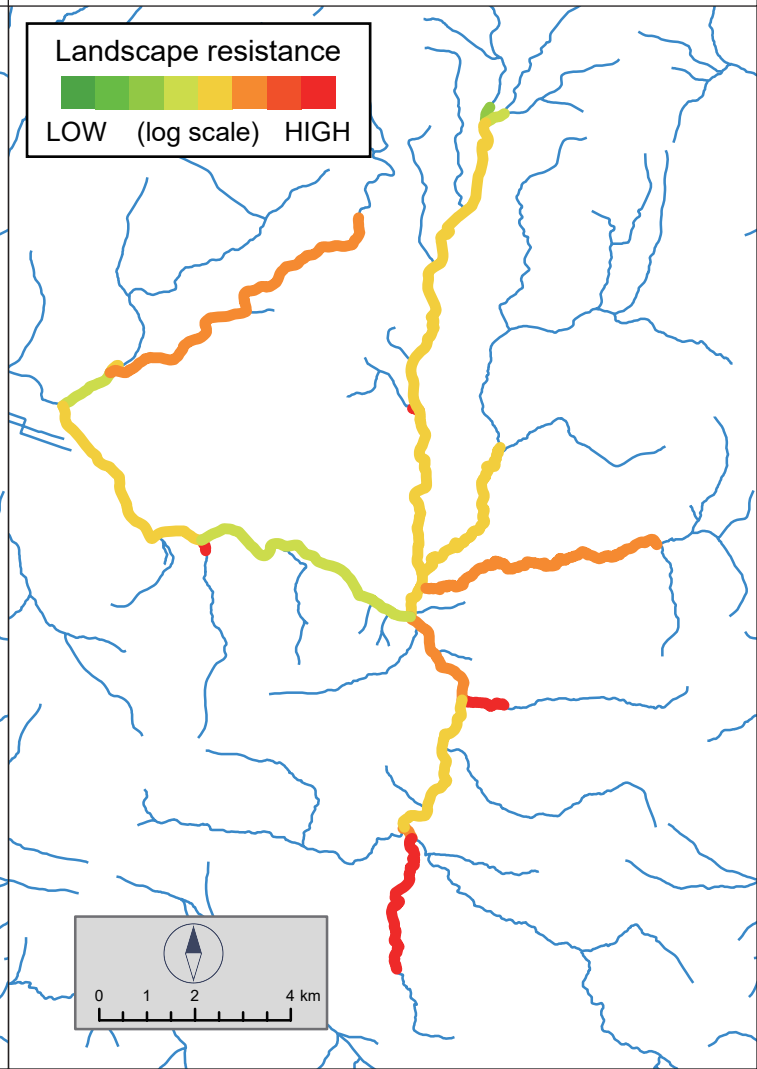
557

558 **Fig. 3** Isolation by distance and isolation by resistance. The relationship between pairwise genetic  
 559 distance and cumulative landscape resistance between populations (b, d) is compared to the  
 560 relationship with simple waterway geographic distance (a, c). The cases of  $G_{ST}$  (a, b) and  $D_{PS}$  (c, d) are  
 561 shown.

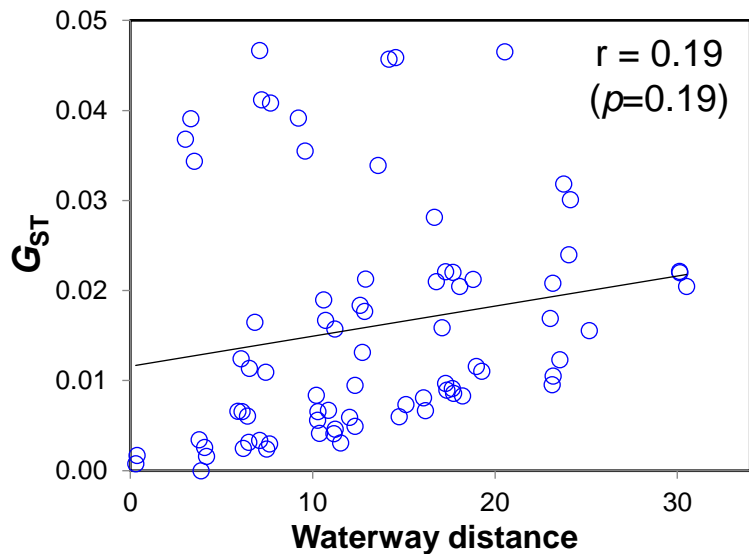
562



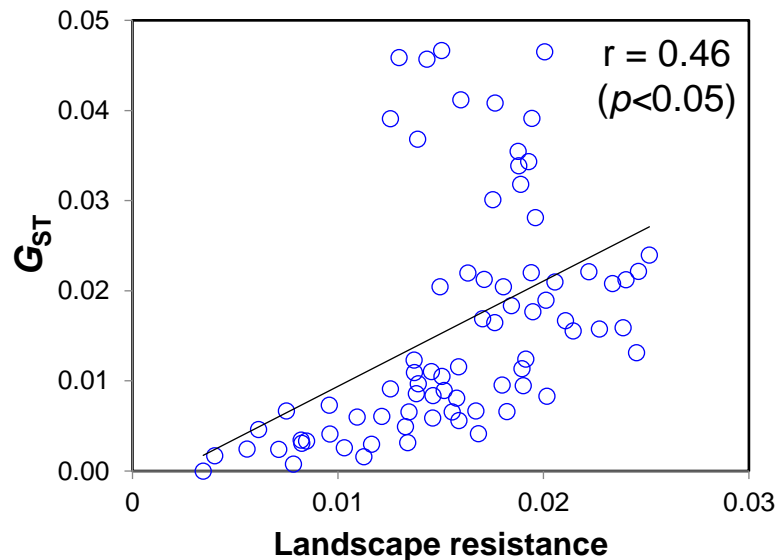


**(a) Study sites****(b) Long-term (based on  $G_{ST}$ )****(c) Current (based on  $D_{PS}$ )****(d) Future (at the end of 21C)**

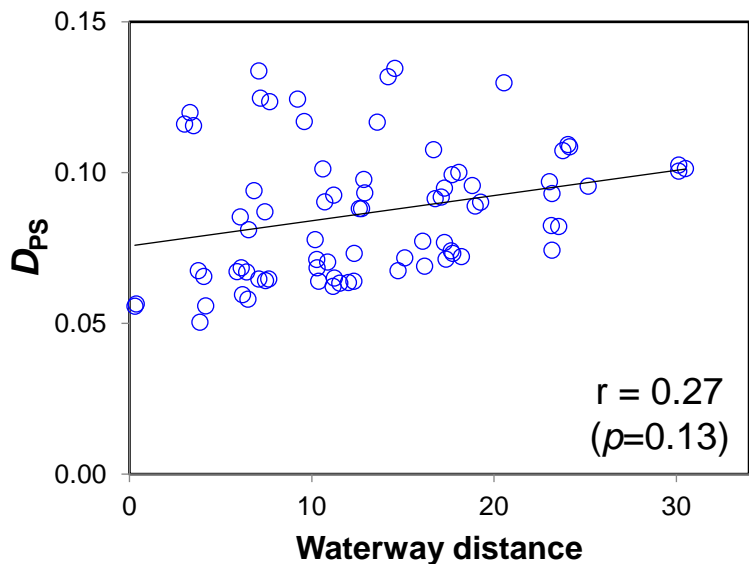
**(a)**  $G_{ST}$  - Isolation by distance



**(b)**  $G_{ST}$  - Isolation by resistance



**(c)**  $D_{PS}$  - Isolation by distance



**(d)**  $D_{PS}$  - Isolation by resistance

